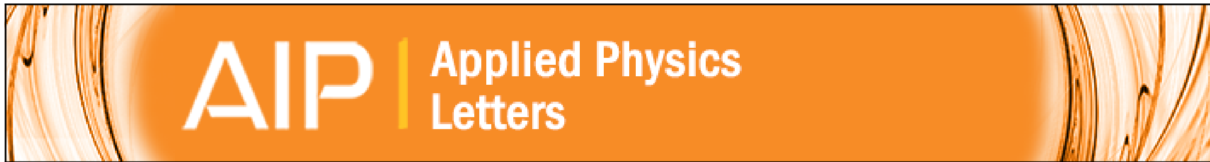

Contact-induced defect propagation in ZnO

J. E. Bradby, S. O. Kucheyev, J. S. Williams, C. Jagadish, M. V. Swain, P. Munroe, and M. R. Phillips

Citation: Applied Physics Letters **80**, 4537 (2002); doi: 10.1063/1.1486264
View online: http://dx.doi.org/10.1063/1.1486264
View Table of Contents: http://scitation.aip.org/content/aip/journal/apl/80/24?ver=pdfcov
Published by the AIP Publishing

Articles you may be interested in
Yielding and plastic slip in ZnO
Appl. Phys. Lett. **100**, 211903 (2012); 10.1063/1.4720169

Structural recovery of ion implanted ZnO nanowires
J. Appl. Phys. **111**, 083524 (2012); 10.1063/1.4704697

Defect properties of ZnO and ZnO:P microwires
J. Appl. Phys. **109**, 013712 (2011); 10.1063/1.3530610

Observation of enhanced defect emission and excitonic quenching from spherically indented ZnO
Appl. Phys. Lett. **89**, 082102 (2006); 10.1063/1.2338552

Mechanical properties of ZnO epitaxial layers grown on a - and c -axis sapphire
Appl. Phys. Lett. **86**, 203105 (2005); 10.1063/1.1929874

AIP | APL Photonics
APL Photonics is pleased to announce Benjamin Eggleton as its Editor-in-Chief

This article is copyrighted as indicated in the article. Reuse of AIP content is subject to the terms at: http://scitation.aip.org/termsconditions. Downloaded to IP: 130.56.106.27 On: Tue, 20 Oct 2015 05:52:29

Contact-induced defect propagation in ZnO

J. E. Bradby,[a)] S. O. Kucheyev, J. S. Williams, and C. Jagadish
Department of Electronic Materials Engineering, Research School of Physical Sciences and Engineering, The Australian National University, Canberra, ACT 0200, Australia

M. V. Swain
Biomaterials Science Research Unit, Department of Mechanical and Mechatronic Engineering and Faculty of Dentistry, The University of Sydney, Eveleigh, NSW 1430, Australia

P. Munroe
Electron Microscope Unit, University of New South Wales, Sydney, NSW 2052, Australia

M. R. Phillips
Microstructural Analysis Unit, University of Technology, Sydney, Broadway, NSW 2007, Australia

(Received 5 February 2002; accepted for publication 23 April 2002)

Contact-induced damage has been studied in single-crystal (wurtzite) ZnO by cross-sectional transmission electron microscopy (XTEM) and scanning cathodoluminescence (CL) monochromatic imaging. XTEM reveals that the prime deformation mechanism in ZnO is the nucleation of slip on both the basal and pyramidal planes. Some indication of dislocation pinning was observed on the basal slip planes. No evidence of either a phase transformation or cracking was observed by XTEM in samples loaded up to 50 mN with an $\sim$4.2 μm radius spherical indenter. CL imaging reveals a quenching of near-gap emission by deformation-produced defects. Both XTEM and CL show that this comparatively soft material exhibits extensive deformation damage and that defects can propagate well beyond the deformed volume under contact. Results of this study have significant implications for the extent of contact-induced damage during fabrication of ZnO-based (opto)electronic devices. © *2002 American Institute of Physics.* [DOI: 10.1063/1.1486264]

There is considerable interest in wide-band-gap II–VI semiconductors as potential materials for the fabrication of short-wavelength (opto)electronic devices such as blue light-emitting diodes and laser diodes. Zinc oxide is currently an attractive II–VI material as a result of recent advances in the production of high-quality single crystals.[1,2] Apart from a direct wide-band gap, ZnO also exhibits a variety of other attractive properties for potential device manufacture such as the possibility of wet-chemical processing, a large exciton binding energy, and a low-power threshold for optical pumping.[1,2] Furthermore, it has been suggested that ZnO may provide an ideal substrate for GaN epilayer growth, as the lattice mismatch between ZnO and GaN is only 2.2% (compared with a mismatch of 16% for GaN grown on a sapphire substrate).[1] Of paramount importance in the manufacture of (opto)electronic devices is the mechanical behavior of the material since fabrication processes involve extensive handling. Indeed, poor mechancial performance of ZnO may severely limit its potential applications since very soft materials may not be compatible with current semiconductor processing. Nanoindentation is an ideal method for studying not only mechanical properties, but also contact-induced damage. In particular, this technique produces highly localized deformation, typical of that obtained during semiconductor handling.

Most previous studies of the mechanical properties of ZnO have been conducted using pointed indenters on polycrystalline material and have provided limited information about the deformation mechanisms.[3–6] A recent nanoindentation study of single-crystal ZnO observed slip steps by atomic-force microscopy (AFM) within residual indent impressions and, hence, identified slip as a major deformation mechanism.[7] This study also reported that single-crystal ZnO is a comparatively "soft" material with a hardness of only $\sim$5 GPa (compared to $\sim$12 GPa for Si and $\sim$15 GPa for GaN). In this letter, we investigate the deformation microstructures formed by contact damage in single-crystal ZnO. Moreover, we discuss the observed correlation of microstructural changes with the nanoindentation load–unload data. Finally, we highlight the important technological implications of our results which reveal that contact-induced defects in ZnO can propagate significant distances in this soft material.

The bulk wurtzite (0001) ZnO samples used in this study were purchased from Cermet Inc.[1] A series of continuous load–unload nanoindentations was made at loads of up to 200 mN with an Ultra Micro Indentation System 2000 (UMIS) at room temperature and atmospheric pressure. A spherical indenter of an $\sim$4.2 μm radius was used throughout this study. Both the UMIS and indenter tip were calibrated using a fused silica standard of known material properties. After indentation, the contact-induced defect microstructures were analyzed using both cross-sectional transmission electron microscopy (XTEM) and scanning cathodoluminescence (CL) monochromatic imaging. The CL study was performed at room temperature using an Oxford Instruments MonoCL2 system, installed on a JEOL 35C scanning electron microscope. Samples for XTEM were prepared using an FEIxP200 focused-ion beam (FIB) system with 30 keV Ga ions. Prior to FIB milling, the samples were

[a)]Electronic mail: jodie.bradby@anu.edu.au

This article is copyrighted as indicated in the article. Reuse of AIP content is subject to the terms at: http://scitation.aip.org/termsconditions. Downloaded to IP: 130.56.106.27 On: Tue, 20 Oct 2015 05:52:29

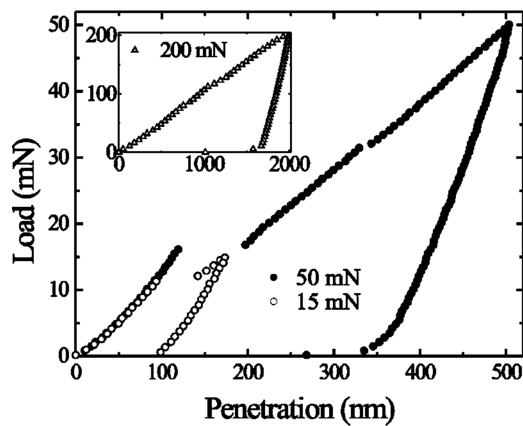

FIG. 1. Load–penetration curves of ZnO indented to maximum loads of 15 and 50 mN. Inset: load–penetration curve of ZnO to a maximum load of 200 mN.

mechanically polished to a thickness of ~60 μm. To protect the surface during the ion milling process, an ~1-μm-thick layer of Pt was deposited over the surface using the FIB instrument. The transmission electron microscope used in this study was a Philips CM 300 operated at an accelerating voltage of 300 kV.

Figure 1 shows the nanoindentation loading curves from ZnO indented to maximum loads of 15, 50, and 200 mN (inset). The maximum depths of indenter penetration are ~175, 500, and 2000 nm for the 15, 50, and 200 mN indents, respectively, indicating that ZnO is relatively soft, as previously observed.[7] All loading curves show characteristic discontinuities ("pop-in" events) on loading, with multiple pop-in events routinely observed for maximum loads above 15 mN.[7] These pop-in events are characteristic of catastrophic plastic deformation as a result of structural changes induced by nanoindentation.[7,8] Previous XTEM studies of other semiconductor materials have revealed a number of plastic deformation mechanisms occurring as a result of mechanical loading by nanoindentation, including densification by phase transformation and slip by punching out of dislocation arrays.[8–10] It is, therefore, interesting to examine the prime modes of plastic deformation in ZnO.

A bright-field XTEM image of an indent made with a maximum load of 15 mN is shown in Fig. 2. Even at this relatively low maximum load, an extensive array of deformation-induced defects is apparent, but no cracking is observed. Slip on the {0001} basal planes along with dislocations aligned ~60° to the surface can be seen. These dislocations are most likely on the $\{10\bar{1}1\}$ (pyramidal) planes. Similar slip patterns have been observed in other hexagonal systems.[10] Selected area diffraction patterns of the mechanically damaged regions directly beneath the indenter, in the region of greatest hydrostatic stress, were carefully studied and showed no evidence of structural transformations to other phases of ZnO. Although densification by phase transformation (to a NaCl structure with a 16% volume change) has been observed in diamond anvil cell experiments in ZnO,[11] the hydrostatic pressure needed to obtain this change is 10 GPa. This is well above the maximum pressure realized in this study (<6 GPa) before plastic deformation is observed.[7] The maximum contact diameter at this load is ~2.4 μm (calculated from the measured indenter radius and depth of penetration). The diameter of the damaged region shown in this image is ~2 μm, suggesting that the XTEM-visible defects remain within the residual indent impression. Further, it is interesting to note that the region of maximum shear stress under the indenter[11] is located just ~0.5 μm beneath the surface, yet Fig. 2 shows defects extending almost an order of magnitude further down (>3 μm) into the bulk. This suggests that the indentation-induced defects initiated in this region of high shear stress are able to propagate a considerable distance in ZnO, the significance of which is discussed below.

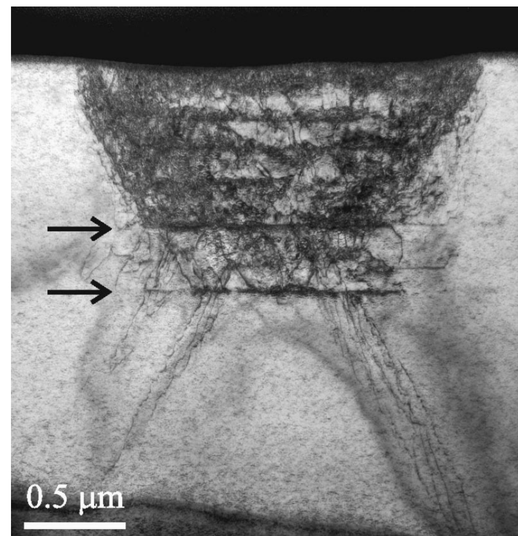

FIG. 2. Bright-field XTEM image of a spherical indent in ZnO at a maximum load of 15 mN. Arrows denote slip bands along the basal planes which result in pinning.

An indent at a higher maximum load of 50 mN is shown in the bright-field XTEM image in Fig. 3. Dense arrays of indentation-induced defects can be seen directly under the clearly visible residual indent impression, which has a contact diameter of ~3.3 μm. The deformation microstructure at this higher load appears similar to that of the lower-load 15 mN indent (Fig. 2), with extensive slip along the basal and pyramidal planes. Apparent in the image of the higher-load indent in Fig. 3 are the high contrast horizontal bands arising from abrupt changes in the density of defects at slip bands aligned along the basal planes (denoted by arrows).

A comparison of the XTEM images in Figs. 2 and 3

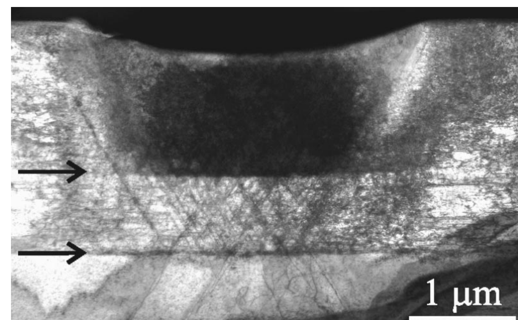

FIG. 3. Bright-field XTEM image of a spherical indent in ZnO at a maximum load of 50 mN. Arrows denote slip bands along the basal planes which result in pinning. Note: darker region in the bottom-right-hand corner is due to increased sample thickness caused by the "folding" over of thin layers during the FIB milling process.

This article is copyrighted as indicated in the article. Reuse of AIP content is subject to the terms at: http://scitation.aip.org/termsconditions. Downloaded to IP: 130.56.106.27 On: Tue, 20 Oct 2015 05:52:29

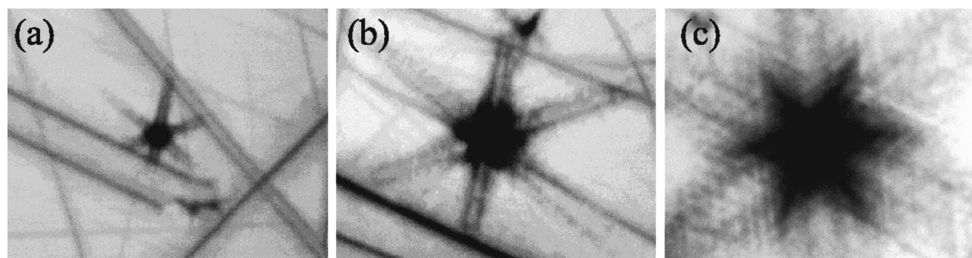

FIG. 4. Room-temperature monochromatic CL images of spherical indents in ZnO. The maximum loads are (a) 15 mN, (b) 50 mN, and (c) 200 mN. The field widths are ~65 μm for all three images. Note additional dark bands extending across the samples appear to be associated with remnant damage caused by mechanical polishing during manufacture. CL imaging conditions: electron-beam energy = 20 keV, CL wavelength = 376 nm, and CL bandpass = 2.5 nm.

reveals several interesting processes which evolve with increasing load. The spacing of the dense bands of defects along the basal planes suggests that, once slip is nucleated, further loading favors continued slip within these previously nucleated bands, rather than defect nucleation and propagation deeper into the material. However, with further loading, stresses build up at greater depths, and it is now energetically favorable for nucleation of slip to occur in bands deeper in the material. In addition, higher loads (see Fig. 3) cause similarly extensive slip in bands along pyramidal planes at ~60° to the surface. We speculate that the high contrast slip bands along basal planes act as pinning sites for defect propagation, particularly deeper into the material. Note the progressively lower density of defects with increasing depth between successive basal slip bands (arrowed in Fig. 3). Such a pinning mechanism can explain the multiple pop-in events[7] observed in the higher load curves shown in Fig. 1, whereby pinning of defects allows stress to build up with increasing load until the onset of further slip occurs in a band deeper in the material. Another possible consequence of the pinning of defects, which propagate into the material by the horizontal slip bands, is that strain energy may be more favorably released by the nucleation and propagation of defects laterally. Indeed, defects are observed to extend out radially across the entire ~20 μm electron transparent region for the 50 mN indent shown in Fig. 3.

The extent of the radial propagation of contact-induced defects can also be clearly seen in Fig. 4, which shows a series of CL images of indents corresponding to the maximum loads in Fig. 1. All three images show dramatic suppression of CL near-gap emission from central regions of the residual indent impressions, the extent of which increases with increasing load. This quenching can be observed to extend radially out from the center of the indent along axes at 60° intervals, characteristic of the hexagonal crystal system. In the case of the 50 mN indent, these damage bands extend out up to ~30 μm from the center of the indent, a trend which is consistent with the XTEM observations of extended defects as discussed above. It is interesting to note that the earlier CL studies of indents in GaN—a structurally similar material—did not find a quenching of luminescence much beyond the indenter contact diameter.[12,13]

The extensive propagation of defects beyond the point of contact in ZnO is of significant relevance to the removal of polishing disorder on ZnO wafers and to the wafer handling during the manufacture of devices. This situation is unlike other III–V compound semiconductors such as GaN,[13] where such extensive damage does not occur as a consequence of wafer handling. Further evidence for extensive wafer handling damage in ZnO is illustrated in Fig. 4 by the dark lines that are observed to extend across the entire sample. These lines, which indicate strong suppression of CL emission, are not associated with the indentation-induced damage. We believe that these defective regions may arise from polishing damage which has not been completely removed by subsequent chemical polishing of the surface. Indeed, the lines clearly observed in Fig. 4 are not readily observable in either AFM or XTEM, and may possibly be caused by residual defects from surface scratches. This indicated that CL imaging is more sensitive to such residual defects which may consist of point-defect clusters rather than extended defects.

In conclusion, this work has enabled the mechanical deformation structures in single-crystal ZnO to be identified. The major mechanism for contact-induced deformation is the sudden and catastrophic nucleation and propagation of slip along the pyramidal and basal planes. Due to the soft nature of this material, relatively small loads result in significant mechanical damage which extends deep into the bulk of the material and laterally well beyond the residual indent impression. Moreover, quenching of CL emission is not only observed to result from indentation-induced disorder but also from remnant mechanical damage produced during wafer polishing. The possible generation of such deeply propagating defects needs to be taken into account in wafer handling and manufacture of ZnO-based devices.

[1] J. E. Nause, III–V Rev. **12**, 28 (1999).
[2] D. C. Look, Mater. Sci. Eng., B **80**, 383 (2001).
[3] S. V. Prasad and J. S. Zabinski, Wear **203-204**, 498 (1997).
[4] M. J. Mayo, R. W. Siegel, Y. X. Liao, and W. D. Nix, J. Mater. Res. **7**, 973 (1992).
[5] V. R. Regel *et al.*, Cryst. Res. Technol. **17**, 1579 (1982).
[6] J. S. Ahearn, J. J. Mills, and A. R. C. Westwood, J. Appl. Phys. **49**, 96 (1977).
[7] S. O. Kucheyev, J. E. Bradby, J. S. Williams, C. Jagadish, and M. V. Swain, Appl. Phys. Lett. **80**, 956 (2002).
[8] T. F. Page, L. Riester, and S. V. Hainsworth, Mater. Res. Soc. Symp. Proc. **522**, 113 (1998).
[9] J. E. Bradby, J. S. Williams, J. Wong-Leung, M. V. Swain, and P. Munroe, J. Mater. Res. **16**, 1500 (2001).
[10] J. E. Bradby, S. O. Kucheyev, J. S. Williams, J. Wong-Leung, M. V. Swain, P. Munroe, G. Li, and M. R. Phillips, Appl. Phys. Lett. **80**, 383 (2002).
[11] D. Tabor, *The Hardness of Metals* (Oxford University Press, Oxford, U.K., 1951).
[12] M. H. Zaldivar, P. Fernandez, and J. Piqueras, Semicond. Sci. Technol. **13**, 900 (1998).
[13] S. O. Kucheyev, J. E. Bradby, J. S. Williams, C. Jagadish, M. Toth, M. R. Phillips, and M. V. Swain, Appl. Phys. Lett. **77**, 3373 (2000).

This article is copyrighted as indicated in the article. Reuse of AIP content is subject to the terms at: http://scitation.aip.org/termsconditions. Downloaded to IP: 130.56.106.27 On: Tue, 20 Oct 2015 05:52:29